Available online at www.sciencedirect.com
SCIENCE DIRECT®
European Polymer Journal 40 (2004) 927–932
EUROPEAN POLYMER JOURNAL
www.elsevier.com/locate/europolj

Jumping mode atomic force microscopy obtains reproducible images of Alzheimer paired helical filaments in liquids

F. Moreno-Herrero [a,*], J. Colchero [a], J. Gómez-Herrero [a], A.M. Baró [a], J. Ávila [b]

[a] *Laboratorio de Nuevas Microscopías, Facultad de Ciencias, C-III, 205, Departamento de Física de la Materia Condensada, Universidad Autónoma de Madrid, Cantoblanco, E-28049 Madrid, Spain*

[b] *Centro de Biología Molecular "Severo Ochoa" (UAM-CSIC), Facultad de Ciencias, Universidad Autónoma de Madrid, 28049 Madrid, Spain*

Received 11 July 2003; received in revised form 15 December 2003; accepted 20 January 2004

Abstract

Alzheimer paired helical filaments (PHF) have been investigated with atomic force microscopy (AFM) under physiological conditions. Dynamic mode (DM) and jumping mode (JM) AFM have been employed as imaging techniques. Data obtained in solution have been compared to data obtained in ambient air with DM. In liquids, PHF particles show distortion and irreversible damage when imaged with DM. On the contrary, JM images of PHF particles are reproducible and out of apparent damage. Dimensions of the PHF particles measured with JM, are in agreement with previously reported electron microscopy data. We have found that the forces involved in DM imaging are larger than those involved in JM imaging and hence we believe that this is the main reason of the damage caused by the tip when using DM in solution.

Keywords: Atomic force microscopy; Paired helical filaments; Tau protein; Jumping mode

1. Introduction

Atomic force microscopy (AFM) [1] makes it possible to image the surface of samples on a nanometer scale in ultrahigh vacuum, ambient air and liquids. During the past decade we have witnessed a spectacular growth of the applications of AFM to the study of biological molecules. AFM is, nowadays, a well-known technique that routinely obtains images of biological samples like DNA [2], DNA and proteins [3,4], viruses [5], protein assemblies [6], antibodies [7], etc. In fact, AFM has been used, not only to image a wide variety of biological samples but also, to perform single molecule experiments [8–11].

Alzheimer's disease (AD) is a senile dementia. Histopathological analysis of the brain of AD patients have indicated the presence of two aberrant structures: extracellular senile plaques (SP) and intracellular neurofibrillary tangles (NFT). NFT are composed of bundles of filamentous structures [12] termed paired helical filaments (PHF) [13]. Several groups have indicated that the microtubule associated protein tau is the major component of PHF [14–16] and that PHF-like polymers could be assembled under different conditions by using tau as the unique protein component [17–22]. PHF structure have already been investigated with AFM in ambient air [23,24].

We have used dynamic mode (DM) [25,26] and jumping mode (JM) AFM [27–29] to study PHF under physiological conditions. DM is the most used AFM

* Corresponding author. Tel.: +34-91-3974754; fax: +34-91-3973961.

E-mail address: fernando.moreno@uam.es (F. Moreno-Herrero).

0014-3057/$ - see front matter © 2004 Elsevier Ltd. All rights reserved.
doi:10.1016/j.eurpolymj.2004.01.018

imaging mode and its advantages for imaging a wide variety of samples in ambient air are well accepted by the scientific community. However, in liquids, the most appropriate imaging mode is not clear yet. In this work, we study which technique provides best results imaging PHF particles in liquids under standard operating conditions. Data obtained in solution have been compared to that obtained in air using DM. PHF are described as left handed helical structures with an average pitch of 70 nm and a variable width between 10 and 20 nm as reported from electron microscopy images [30]. We have found that, in liquids, best results are obtained using JM.

2. Experimental

2.1. AFM sample preparation

PHF samples were prepared adapting the protocol described in [24] for imaging in liquids. After an adsorption time of 5 min, the mica was placed in a liquid cell and filled with 1 ml of 0.01 M Phosphate Buffered Saline pH 7.4 (PBS) (Sigma-Aldrich, Alcobendas, Spain). Molecules imaged in liquid were never allowed to dry.

2.2. Dynamic mode

When operating the AFM in DM, the cantilever is oscillated near its free resonance frequency, then the sample is approached to the surface until the amplitude of the cantilever is reduced to the set point value. Tip–sample interaction produces a strong amplitude reduction when the tip–sample gap is in the nanometer range. The tip is then scanned over the surface while the feedback mechanism measures and keeps constant the oscillation amplitude.

Olympus type cantilevers with a force constant of 0.75 N/m were used with DM. The resonance frequency in liquid operation was 22 kHz. DM images were obtained using typical amplitude oscillations of 10–80 nm and scan rates of 3–7 lines per second.

2.3. Jumping mode

JM works by performing a sequence of force versus distance curves at each point of the sampled surface with a feedback time in between. First, the tip is in contact with the surface while the feedback is keeping the cantilever deflexion at the set point. Then the feedback is turned off and the tip is vertically moved away from the surface. At maximum tip–sample separation, the tip is moved laterally to the next point avoiding lateral forces. Finally, the tip is brought again into contact with the surface. Hence, in JM the feedback signal is the cantilever's deflection. This situation can be contrasted with DM where the feedback signal is the oscillation amplitude of the cantilever.

For JM we have used Nanosensors type cantilevers of constant force 0.02 N/m (NanosensorGmbH & Co, KG). A comparison between DM and JM and a detailed description of the experimental conditions used in both imaging modes can be found in [31].

3. Results and discussion

PHF have been investigated using DM and JM in ambient air and in solution. Data are shown in Fig. 1. In ambient air, best results are obtained using DM (Fig. 1(A) and (B)). Filamentous structures can be identified from AFM images. These structures are attributed to PHF particles. PHF appear as left handed filaments with a pitch of 75 nm in agreement with previous electron microscopy [30] and AFM results [23,24]. Straight filaments are also possible [32] and can be also found in DM AFM images (see arrow in Fig. 1(A)). A high magnification image of a PHF is shown in Fig. 1(B). A longitudinal profile of a PHF particle is depicted in the inset. Typical heights of PHF are 15 nm for the highest points and 10 nm for the lowest. The helical structure of PHF is clear since the difference in height from top to low points is high (about 5 nm). JM is useless for imaging PHF in ambient air due to high adhesion forces ($\sim$10 nN).

Imaging in solution is much harder than in air. There is a set of technical issues which arise when working in liquids. Samples are placed in a liquid cell that must ensure isolation from piezoelectric voltages. Also, the cantilever must be oscillated when using DM. This can be done by moving the whole liquid cell where the cantilever is held using a piezo-acoustic drive oscillator (acoustic DM) [25] by moving the cantilever using a magnetic field (magnetic DM) [33]. In the latter case a magnetic material must be evaporated on the cantilever. Data showed in this work were obtained using acoustic DM. Sample preparation is probably the main concern. Molecules must be firmly attached to the substrate in order to be imaged but not too much in order to avoid structure distortion. In addition tip–sample interaction must be always weaker than sample–substrate interaction.

DM and JM images of PHF in solution are shown in Fig. 1(C), (D) and (E), (F), respectively. A few molecules can be identified in the low magnification image obtained with DM (Fig. 1(C)). Since sample concentration was similar to that of the JM experiment we conclude that most of the PHF particles were moved by the scan when using DM. A high magnification image of a PHF obtained with DM is shown in Fig. 1(D). The filament shows irreversible damage and distortion. Maximum

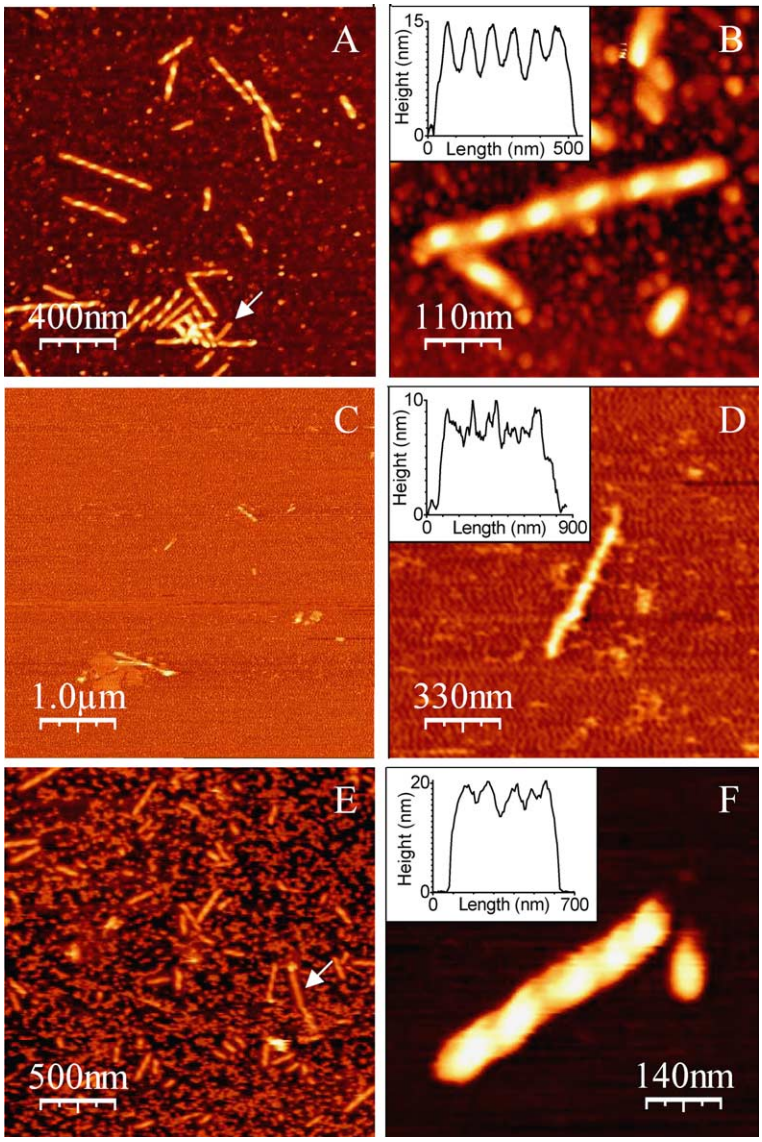

Fig. 1. AFM images of Alzheimer paired helical filaments. Images shown in (A) and (B) were obtained in ambient air using DM. Images acquired in solution with DM are shown in (C) and (D) and with JM in (E) and (F). Characteristic PHF profiles for each imaging mode and environment are displayed in the insets of (B, D and F).

height is 10 nm. This value is much lower than that measured in air using the same technique. In addition, longitudinal periodicity can be hardly resolved. In contrast with DM results, JM images of PHF particles in liquids show an acceptable resolution and non-intrusiveness. JM images are shown in Fig. 1(E) and (F). PHF have a maximum height of 20 nm and a minimum height of 15 nm. The maximum height is in agreement with electron microscopy data previously reported [32]. Helical periodicity is 70 nm. Molecules in liquids appear more compact than in air as expected.

In contrast with the situation in ambient air where DM operation can be done in contact or non-contact regimes, in liquids, contact between tip and sample cannot be avoided [34,35]. Fig. 2 shows the normal force (deflection) versus distance when operating DM and JM in liquids.

Fig. 2(A) is related with DM operation. Tip is oscillated near its resonance frequency which, in liquids, is about 22 kHz at amplitudes ranging 10–80 nm. The average normal force versus distance is also plotted. Note that at soon as the amplitude decreases, a non-zero

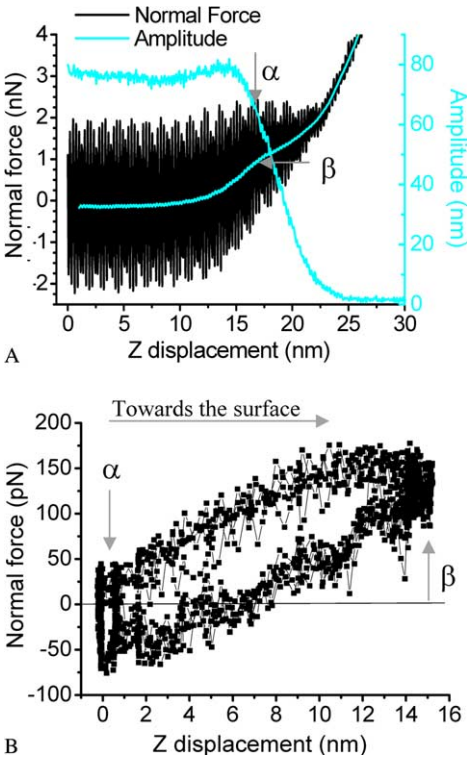

Fig. 2. Normal force versus distance plots at DM (A) and JM (B) operating conditions in liquids. In (A), the amplitude signal of the cantilever movement and the average normal force are also displayed. DM images were obtained at 10% reduction of the free amplitude (point α). This amplitude reduction corresponds to an average force of ~1 nN (point β). In (B) several force versus distance cycles are plotted together. Note the absence of adhesion force and the hysteresis of the cycle due to viscous drag of the cantilever in the surrounding liquid. Point α corresponds to the zero force level where tip is out of contact. Point β corresponds to the set point. Images were obtained at a fixed force of 150 pN.

average normal force appears. This is in contrast with the situation in ambient air [36]. Images were taken at a 10% reduction in amplitude (point α) which corresponds to an average force of ~1 nN (point β).

Fig. 2(B) shows a set of force versus distance curves in liquids when operating JM. The cycle presents a characteristic hysteresis due to drag of the surrounding liquid by the cantilever. Lower loop corresponds to the indentation movement of the tip and upper loop to the retrace process. Tip is free of short-range interactions at point α. At this point the measured normal force is zero. When the tip is approached to the sample surface, a continuous change in the normal force takes place. The movement of the Z piezo continues until a selected force is reached (point β). Images were obtained at a normal force of 150 pN.

Biological material is characterized by its softness. For this reason, imaging of bio-samples can only be achieved at very low forces. It has been claimed that forces larger than 100 pN are destructive when imaging crystal polymers [37]. A main difference between DM and JM is the control parameter. In DM, the feedback channel is the amplitude of the oscillation and in JM, the control channel is the normal force. In addition, the absence of adhesion force in liquids allows small Z excursions to move the tip in and out of contact. Note that the oscillation amplitude in DM and the Z excursion in JM in liquids are of the same order of magnitude in contrast with the situation in ambient air. Typical JM image time in liquids is 3 min. In ambient air, the presence of capillary forces implies a much larger Z movement of the piezo in JM operation. Large Z movement increases time acquisition and hence JM in air is slow which is a main drawback. Typical JM image time in air is 6 min. In liquids, a precise control of the applied force is essential and this is only done when using JM.

PHF is a soft polymer of protein tau. Results show that these filaments can only be imaged at high resolution in liquids using JM under the experimental conditions described above. Fig. 2 shows that applied forces in DM are much larger than those applied in JM. We believe that this is the main cause of the low resolution and the irreversible damage shown in DM images of PHF. We have taken images with JM at larger forces and then PHF particles are broken and cut (data not shown). This happens at forces larger than 500 pN.

4. Conclusion

Alzheimer PHF, a polymer of the microtubule associated protein tau, have been investigated with AFM. Data obtained in air with DM show PHF particles as left handed helical filaments with a variable height between 10 nm and 15 nm. PHF samples have been also investigated in solution using DM and JM. DM data show filamentous structures with clear degradation and low heights. JM allows to obtain reproducible images of PHF particles with high resolution. Measured heights are in agreement with electron microscopy reported data. A detailed analysis of the normal forces involved in the process of image acquisition shows that the force applied by the tip when using DM is larger than that applied when using JM. The large normal force applied with DM in liquids is the cause of the damage reported in the PHF images. In principle imaging with DM at lower forces is possible if softer cantilevers are employed. But then, scanning rate dramatically drops since actual soft cantilevers have low resonance frequencies. The resonance frequency can be increased by reducing cantilever's dimensions [38]. Future fast and soft imag-

ing of biomolecules will be possible using small cantilevers. Nowadays, JM can be superior to DM when imaging individual isolated biological macromolecules as have been seen when imaging Alzheimer PHF.

Acknowledgements

We acknowledge support from the Comunidad de Madrid through a Ph.D. fellowship for F. Moreno-Herrero. This work is supported by the Ministerio de Educación y Cultura through a DGESIC project No. BFM2001-0150, MAT2001-0664 and MAT2002-01084.

References

[1] Binnig G, Quate CF, Gerber C. Atomic force microscope. Phys Rev Lett 1986;56(9):930.
[2] Hansma HG. Surface biology of DNA by atomic force microscopy. Annu Rev Phys Chem 2001;52:71.
[3] Moreno-Herrero F, Herrero P, Colchero J, Baro AM, Moreno F. Imaging and mapping protein-binding sites on DNA regulatory regions with atomic force microscopy. Biochem Biophys Res Commun 2001;280(1):151.
[4] Bussiek M, Klenin K, Langowski J. Kinetics of site–site interactions in supercoiled DNA with bent sequences. J Mol Biol 2002;322(4):707.
[5] Kuznetsov YG, Malkin AJ, Lucas RW, Plomp M, McPherson A. Imaging of viruses by atomic force microscopy. J Gen Virol 2001;82(Pt 9):2025.
[6] Mou J, Sheng S, Ho R, Shao Z. Chaperonins GroEL and GroES: views from atomic force microscopy. Biophys J 1996;71(4):2213.
[7] San Paulo A, Garcia R. High-resolution imaging of antibodies by tapping-mode atomic force microscopy: attractive and repulsive tip–sample interaction regimes. Biophys J 2000;78(3):1599.
[8] Rief M, Gautel M, Oesterhelt F, Fernandez JM, Gaub HE. Reversible unfolding of individual titin immunoglobulin domains by AFM. Science 1997;276(5315):1109.
[9] van Noort SJ, van der Werf KO, Eker AP, Wyman C, de Grooth BG, van Hulst NF, et al. Direct visualization of dynamic protein-DNA interactions with a dedicated atomic force microscope. Biophys J 1998;74(6):2840.
[10] Rivetti C, Guthold M, Bustamante C. Wrapping of DNA around the E. coli RNA polymerase open promoter complex. Embo J 1999;18(16):4464.
[11] Kasas S, Thomson NH, Smith BL, Hansma HG, Zhu X, Guthold M, et al. Escherichia coli RNA polymerase activity observed using atomic force microscopy. Biochemistry 1997;36(3):461.
[12] Terry RD, Wisniewski HM. In: Gaitz CM, editor. Aging and brain. New York: Plenum Publishing Corporation; 1972. p. 89.
[13] Kidd M. Paired helical filaments in electron microscopy of Alzheimer's disease. Nature 1963;197:192.
[14] Grundke-Iqbal I, Iqbal K, Tung YC, Quinlan M, Wisniewski HM, Binder LI. Abnormal phosphorylation of microtubule-associated protein tau in Alzheimer cytoskeletal pathology. Proc Natl Acad Sci USA 1986;83:4913.
[15] Wood JG, Mirra SS, Pollock NJ, Binder LI. Neurofibrillary tangles of Alzheimer disease share antigenic determinants with the axonal microtubule-associated protein tau. Proc Natl Acad Sci USA 1986;83:4040.
[16] Kosic KS, Bakalis SF, Selkoe DJ, Pierce MW, Duffy LK. High molecular weight microtubule-associated proteins: purification by electro-elution and amino acid components. J Neurosci Res 1986;15:543.
[17] Montejo de Garcini E, Carrascosa JL, Correas I, Nieto A, Avila J. Tau factor polymers are similar to paired helical filaments of Alzheimer's disease. FEBS Lett 1988;236:150.
[18] Crowther RA, Olesen OF, Smith MJ, Jakes R, Goedert M. Assembly of Alzheimer-like filaments from full length tau protein. FEBS Lett 1994;337:135.
[19] Wille H, Drewes G, Biernat J, Mandelkow EM, Mandelkow E. Alzheimer-like paired helical filaments and antiparallel dimers formed from microtubule-associated protein tau in vitro. J Cell Biol 1992;118:573.
[20] Wilson DM, Binder LI. Free fatty acids stimulate the polymerization of tau and amyloid beta peptides. In vitro evidence for a common effector of pathogenesis in Alzheimer's disease. Am J Pathol 1997;150(6):2181.
[21] Goedert M, Jakes R, Spillantini MG, Hasegawa M, Smith MJ, Crowther RA. Assembly of microtubule-associated protein tau into Alzheimer-like filaments induced by sulphated glycosaminoglycans. Nature 1996;383(6600):550.
[22] Perez M, Valpuesta JM, Medina M, Montejo de Garcini E, Avila J. Polymerization of tau into filaments in the presence of heparin: the minimal sequence required for tau–tau interaction. J Neurochem 1996;67(3):1183.
[23] Pollanen MS, Markiewicz P, Bergeron C, Goh MC. Twisted ribbon structure of paired helical filaments revealed by atomic force microscopy. Am J Pathol 1994;144(5):869.
[24] Moreno-Herrero F, Valpuesta JM, Perez M, Colchero J, Baro AM, Avila J, et al. Characterization by atomic force microscopy and cryoelectron microscopy of tau polymers assembled in Alzheimer's disease. J Alzheimer Disease 2001;3:443.
[25] Martin Y, Williams CC, Wickramasinghe HK. Atomic force microscopy mapping and profiling on a sub 100-A scale. J Appl Phys 1987;61:4723.
[26] Zhong Q, Inniss D, Kjoller K, Elings VB. Fractured polymer/silica fiber surface studied by tapping mode atomic force microscopy. Surf Sci Lett 1993;290:L688.
[27] van der Werf KO, Putman CAJ, Grooth BG, Greve J. Adhesion force imaging in air and liquid by adhesion mode atomic force microscopy. Appl Phys Lett 1994; 65:1195.
[28] Rosa-Zeise A, Weilandt E, Hild S, Marti O. The simultaneous measurement of elastic, electrostatic and adhesive properties by scanning force microscopy: pulsed-force mode operation. Meas Sci Technol 1997;8:1333.
[29] de Pablo PJ, Colchero J, Gómez-Herrero J, Baro AM. Jumping mode scanning force microscopy. Appl Phys Lett 1998;73(22):3300.
[30] Crowther RA, Wischik CM. Image reconstruction of the Alzheimer paired helical filament. EMBO J 1985;4: 3661.

[31] Moreno-Herrero F, de Pablo PJ, Fernández-Sánchez R, Colchero J, Gómez-Herrero J, Baró AM. Scanning force microscopy jumping and tapping modes in liquids. Appl Phys Lett 2002;81:2620.
[32] Crowther RA. Straight and paired helical filaments in Alzheimer's disease have a common structural unit. Proc Natl Acad Sci USA 1991;88:2288.
[33] Han W, Lindsay SM, Jing T. A magnetically driven oscillating probe microscope for operation in liquids. Appl Phys Lett 1996;69(26):4111.
[34] Putman AJ, van der Werf KO, de Grooth B, van Hulst NF, Greve J. Tapping mode atomic force microscopy in liquid. Appl Phys Lett 1994;72:2454.
[35] Hansma PK, Cleveland JP, Radmacher M, Walters DA, Hillner PE, Bezanilla M, et al. Tapping mode atomic force microscopy in liquids. Appl Phys Lett 1994;64:1738.
[36] de Pablo PJ, Colchero J, Luna M, Gomez Herrero J, Baro AM. Tip–sample interaction in tapping-mode scanning force microscopy. Phys Rev B 2000;61(20):14179.
[37] Müller DJ, Fontiadis D, Scheuring S, Müller SA, Engel A. Electrostatically balanced subnanometer imaging of biological specimens by atomic force microscope. Biophys J 1999;76:1101.
[38] Viani MB, Schffer TE, Chand A, Rief M, Gaub HE, Hansma PK. Small cantilevers for force spectroscopy of single molecules. J Appl Phys 1999;84(4):2258.